15TH IEA HEAT PUMP CONFERENCE
MAY 26–29, 2026 | HOFBURG
VIENNA 2026
DECARBONISATION THROUGH INNOVATION

Optimization of Heating Stability During Defrosting in Modular Small-Capacity Air Source Heat Pump Systems

Jian Cao[a], Lingyan Yang[b,c*], Wenju Hu[a], Shuguo Wang[d]

[a]Beijing University of Civil Engineering and Architecture, Beijing 102600, China
[b]China Academy of Building Research, Beijing 100013, China
[c]Jianke EET Co., Ltd., Beijing 100013, China
[d]Hebei Siwei Energy-saving Technology Co., Ltd., Shijiazhuang 050200, China

Abstract

Compared with large-capacity air source heat pump (ASHP) units, modular small-capacity ASHP systems are designed to enhance the stability of water supply temperature under low-temperature and high-humidity conditions by miniaturizing heating units and enabling independent defrost control. However, autonomous defrosting of individual outdoor units can lead to concentrated and periodic group defrosting events, causing significant fluctuations in water supply temperature. This study conducted an 86-day field experiment on a modular ASHP heating system in a cold region of China to analyze the relationship between system defrosting behavior and heating stability. Results showed that when ambient humidity exceeded 80% and compressor frequency was above 70Hz, the system exhibited periodic group defrosting at approximately 2-hour intervals, with a maximum simultaneous defrosting ratio (SDR) of 60% and corresponding temperature drops of 3~4K. Statistical analysis indicated that maintaining the SDR below 25% in high-density defrosting periods or under 60% for instantaneous defrosting events can effectively limit water temperature fluctuations within 3K. Based on these findings, this paper identifies the need for distributed group defrost control in modular ASHP systems and proposes a conceptual framework to limit simultaneous defrosting ratios and eliminate periodic synchronization. Future group-defrost control strategies should incorporate time-staggered scheduling, module-level coordination, and predictive algorithms to achieve distributed defrosting behavior and enhance overall heating resilience of modular ASHP systems.

Keywords: air source heat pump; group defrost control; heating stability

1. Introduction

With the accelerating shift toward clean heating, air-source heat pumps (ASHPs) are widely adopted for their low cost, high efficiency, and ease of deployment. However, severe frosting under low-temperature, high-humidity conditions undermines heating resilience, especially for reverse-cycle defrosting systems where heat is drawn from return water, causing outlet temperature drops. Improving heating stability during defrosting is therefore essential.

Extensive research has addressed this through system structural enhancements, control logic optimization, and mechanistic modeling. Structural improvements enhance defrost efficiency and heating continuity: Li et al. [1] showed thermal-storage-assisted defrosting can improve COP by 3~19.5% at -2~2℃; Yang et al. [2] proposed phase-change energy storage for multi-split heat pumps, significantly enhancing defrosting; Tang et al. [3] maintained 20% heating capacity and reduced defrost time by 40% using partial reverse-cycle defrosting; Zheng et al. [4] stabilized floor and indoor temperatures using phase-change materials in radiant floors; Zhang et al. [5] achieved simultaneous heating and defrosting by coupling radiation–convection terminals; Wei et al.

* Corresponding author. *E-mail address:* yly8111@163.com

15th IEA Heat Pump Conference 2026 - HDU4.1 - https://doi.org/10.23697/eem5-w810

[6] preheated outdoor air to suppress frost, improving COP by 7.4~13.1%; Wu et al. [7] used variable-frequency control to extend frost-free operation and improve system performance by 9%.

Control optimization improves defrost accuracy and energy efficiency: Tang et al. [8] reduced defrost frequency by 39.8% and increased COP by 10.6% using a T-I-T method; Song et al. [9] optimized time-based defrost, achieving 46.05% efficiency at 930 g frost; Miao et al. [10] employed a T-H-I composite method to avoid premature or delayed defrost, reducing energy use by 22.3%; Wang et al. [11] developed a CNN-based model with prediction errors below 12%; Ikram et al. [12] proposed an approach-temperature-based optimal defrost strategy for variable-speed heat pumps.

Mechanistic studies provide theoretical support: Ma et al. [13] simulated alternating frosting and reverse-cycle defrosting; Du et al. [14] highlighted the role of expansion-valve control in defrost reliability; Wang et al. [15] showed higher supply-water temperatures lengthen frost intervals and reduce indoor fluctuations; Song [16] and Ma et al. [17] reviewed anti-frost and defrost technologies, emphasizing the integration of continuous heating and intelligent control.

Overall, these studies indicate a transition from empirical to adaptive, predictive, and intelligent defrost strategies. Yet, most research focuses on single units, neglecting system-level heating stability. Uncoordinated defrosting can cause severe supply-water temperature fluctuations, especially in high-frost-risk conditions. To address this gap, the present study investigates a small-capacity modular ASHP heating system, using field data to evaluate the feasibility and necessity of decentralized group defrost control, providing guidance for future system-level optimization.

The modular small-capacity ASHP system proposed in this paper miniaturizes the regulation units of the heat source, offering several advantages. In terms of defrosting, each small-capacity unit performs autonomous and independent defrosting. Rotational defrosting among units can reduce fluctuations in supply water temperature and ensure heating stability. Additionally, the finer granularity of regulation enables more efficient adaptation to variations in thermal load, thereby improving heating efficiency during partial-load conditions. In low-temperature environments, the two-stage condenser design, which heats water progressively, helps lower the condensation temperature of the first-stage heat pump and enhances overall energy efficiency. Furthermore, the modular system offers flexible installation and easy scalability, generates lower noise, provides greater system redundancy, and through group control, could significantly improve system efficiency, making it easier to deploy in various application scenarios.

2. Methods

2.1. Case Study

To investigate the defrosting stability of small-capacity ASHPs, an 86-day field test was conducted on a residential heating system in a cold region of China. Two identical unit-type systems, System A and System B, were selected for comparative analysis. The system configuration and heat-source layout are shown in Fig. 1. Unlike large-capacity ASHPs, each small-capacity module comprises four heat pump units with independent refrigerant circuits, arranged in two parallel branches with two-stage series heating per branch. A module pump balances water flow, and all modules are connected in parallel on the heat-source side. Both systems use radiant floor heating terminals with parallel indoor loops. A buffer tank on the return-water main stabilizes temperature and hydraulic conditions.

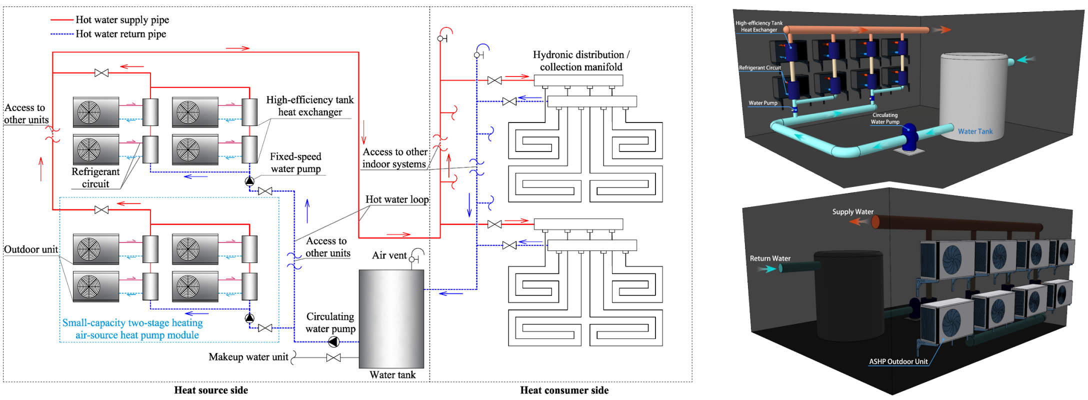

(a) Schematic diagram of the ASHP modules heating system

(b) Schematic diagram of the heat-source side layout

Figure 1. Schematic Diagram of Modular Small-Capacity ASHP System.

The test system consisted of low-temperature-adapted modular air-source heat pump (ASHP) units. Under outdoor 7℃ and outlet water 45℃, each module (composed of four independent ASHPs) had a rated heating capacity of 28 kW, COP of 3.45, and IPLV(H) of 2.95. Direct frequency control (30~120 Hz) was applied, with each module's compressor independently regulated; frequency setpoints and the number of active modules were fixed during operation. Each unit autonomously performed reverse-cycle defrosting using a time–temperature feedback strategy. Defrosting was triggered based on coil surface temperature, defrost temperature, water outlet temperature, and dynamic intervals, with the four-way valve switching and compressors operating at 70 Hz. Termination criteria included coil temperature >24℃ for 10 s, >19℃ for 30 s, defrost duration >10 min, or outlet water temperature <7℃.

Two systems (A and B) were compared: System A with a tightly constrained configuration (10 modules, serving a heated area of 3324 m²) and System B with moderate redundancy (6 modules, serving a heated area of 1675 m²). System A operated continuously at high load, whereas System B allowed more flexible, efficient operation. Indoor setpoints were 18℃, with total heating output adjusted via frequency modulation or number of active modules; unit water flow rates were synchronized. Outdoor and heat-source conditions were consistent, enabling comparative analysis across operating strategies. High-precision instruments ensured reliable data: temperature ±0.3K, relative humidity ±3%, electricity ±0.5%, and heat meters ±2%; measurement and derived errors were within acceptable limits.

2.2. Defrosting Characteristic Indicators

This study analyzes defrosting behavior at both unit and system levels. At the unit level, identifying factors affecting frosting and defrosting intensity is essential for designing optimized decentralized group-defrost control. Defrosting intensity of a unit is represented by R_{def}, the average hourly defrost duration per unit (Equation 1). At the system level, the impact of concentrated and persistent group defrosting on supply-water temperature is quantified using the simultaneous defrost ratio (SDR), defined as the number of units in defrost mode divided by total operating units at each minute. SDR also reflects the proportion of simultaneously defrosting units within a module, enabling analysis of its correlation with inlet–outlet water temperature difference.

$$R_{def} = \frac{\sum_{i=1}^{n} t_i}{60 \times n} \tag{1}$$

where t_i is the total defrosting time (minute) of unit; n is the number of units operating during the statistical period.

3. Results and Discussion

3.1. Defrosting characteristics of ASHP unit

Statistical analysis of unit-level data indicates that, with compressor frequency as the control parameter, 50~75Hz represents the high-efficiency operating range for these heat pumps. Within this range, power consumption increases roughly linearly with frequency, while heating efficiency declines rapidly above 75Hz, which is thus suitable only for short-term supplementary heating under extreme conditions. Accordingly, 75Hz is used as the threshold to analyze frosting characteristics in two frequency ranges.

To quantify factors affecting unit defrosting, a generalized linear model (GLM) was constructed using discretized, normalized data. Outdoor temperature (T_{out}), relative humidity (RH), and operating frequency (f) were independent variables, with hourly defrost ratio (R_{def}) as the dependent variable, including all main and pairwise interaction effects. The model achieved R^2=0.93, RMSE=0.0054, and CV-RMSE=22.3%, demonstrating good predictive accuracy (Equation 2). Since all terms in the regression equation are standardized parameters, the extent of their influence can be quantified by calculating the proportion of the absolute values of each coefficient. Standardized coefficients indicate RH and f dominate, accounting for 77.2% of total influence (Fig. 2b). This indicates that humidity and operating frequency are the most significant factors affecting defrosting based on this defrosting logic.

Correlation analysis between R_{def} and heating degradation shows that humidity is a primary factor (Fig. 2a). When RH<60% and f<65 Hz, R_{def} and degradation remain below 3% and 20%, respectively. In contrast, at RH>80% and f>70 Hz, even R_{def}≈5% (≈3 min/hour) can reduce heating capacity by 50%, highlighting severe efficiency loss. Therefore, under mild outdoor temperatures, reducing operating frequency is recommended to avoid prolonged defrosting and associated performance degradation.

$$logit(R_{def}) = -3.80 - 0.147T_c + 0.632RH_c + 0.379f_c + 0.0512T_cRH_c + 0.149T_cf_c - 0.168RH_cf_c \quad (2)$$

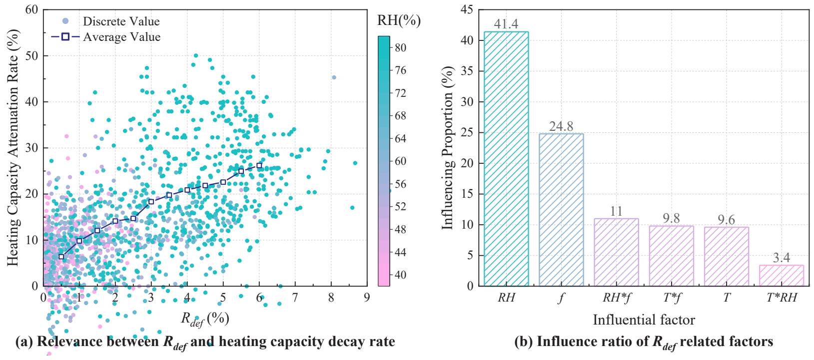

Figure 2. Correlation of Performance Influencing Factors.

At the module level, Fig. 3 shows box-and-whisker distributions of the supply–return water temperature difference (ΔT) under different SDRs for 50~75Hz and 75~95Hz. SDR represents the proportion of simultaneously defrosting units within a module; boxes indicate the 25th–75th percentile range, the line marks the median, and dashed lines show mean ΔT per SDR. Results indicate similar SDR–ΔT trends across both frequency ranges, differing mainly under frost-free conditions. As SDR increases, ΔT gradually decreases, approaching zero near SDR≈50%, suggesting that heat extraction from return water during defrosting is only marginally more efficient than from the outdoor environment in heating mode. Thus, SDR can represent the module's actual heating output ratio. Moreover, SDR and average ΔT are approximately linearly related: each 5% increase in SDR reduces ΔT by 0.48K in 50~75Hz and 0.57K in 75~95Hz.

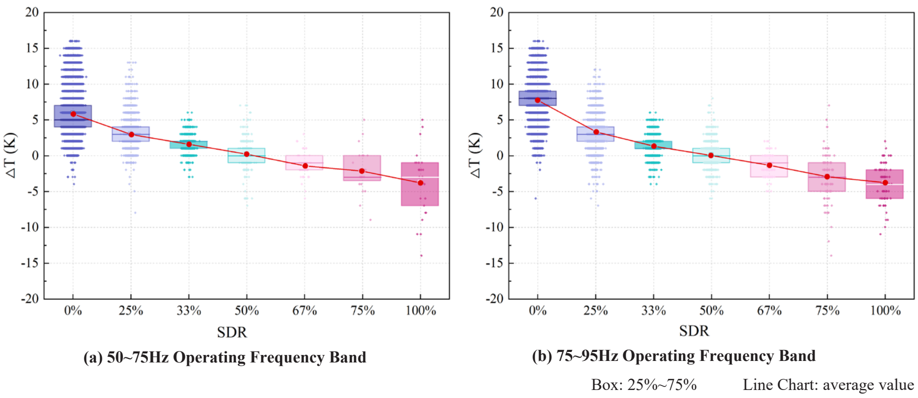

Figure 3. Boxplot of ΔT Distribution as a Function of SDR.

3.2. Defrosting characteristics of ASHP system

Due to the stochastic nature of unit-level defrosting, system-level defrost ratio (SDR) exhibits randomness. To assess its impact on heating stability, this study analyzed system defrosting under unmanaged operation. With a buffer tank stabilizing return-water temperature over short periods, fluctuations in the supply–return temperature difference (ΔT) reflect short-term defrost effects. Figure 4 shows minute-by-minute SDR and total supply–return temperatures for Systems A and B. Higher, more concentrated SDR values correspond to larger short-term ΔT fluctuations, e.g., during early February's high humidity, while ΔT is stable in mid-February. Sudden SDR spikes, even if discrete, can significantly disrupt heating, as seen at January's end.

During high-density defrosting, ΔT fluctuates 2K at SDR=15% and 3K at SDR=25%. For transient defrosts (<3 min), ΔT fluctuates 1K at SDR=40%, 2~3K at SDR=60%, >4K at SDR=80%, and heating nearly fails above SDR=90%. Thus, SDR thresholds can be set: below 15% for high-density periods and below 60% for transient periods to avoid major temperature swings. Additionally, SDR peaks are sporadic "black swan" events, emphasizing the need for decentralized defrost control in heat pump groups to maintain stable heating performance.

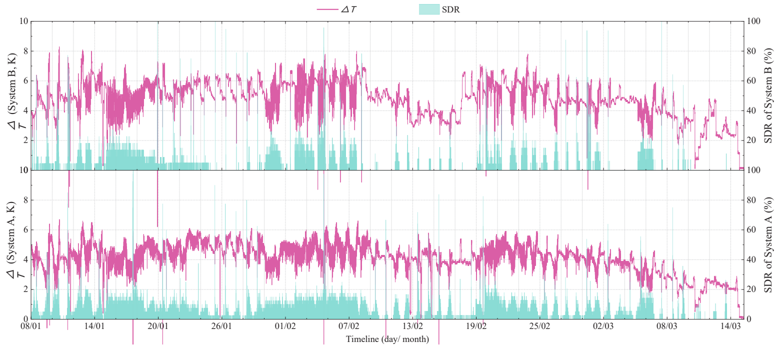

Figure 4. Minute-Scale Time Series of Defrosting Operation.

Test results show that system-level defrosting occurs in segmented, short-duration periods rather than continuously, typically shorter than the time scale of operating condition changes. The stable supply-water temperature before each defrosting period can serve as a baseline to calculate per-minute temperature drops, reflecting the influence of current SDR. Figure 5 shows the correlation between short-term SDR peaks and supply-water temperature drop peaks. Within this range, SDR peaks are generally below 30%, with corresponding temperature drops under 3K. Considering higher SDR fluctuations, maximum limits should also be considered: to avoid short-term drops exceeding 3K, SDR should stay below 25%, or at least under 50%. These results provide practical guidance for developing decentralized defrost control strategies.

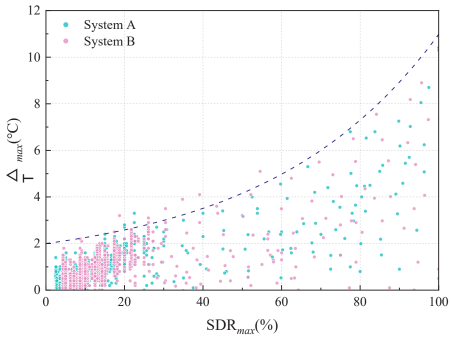

Figure 5. Peaks Correlation between Short-Term SDR and Supply-Return Water Temperature Difference.

3.3. Discussion

Field measurements show that in uncoordinated operation, autonomous unit-level defrosting causes clustered group-level events. When SDR exceeds 25%, supply-water temperature fluctuates over 3K, with periodic concentration under high humidity, reducing the benefits of modular small-capacity systems. Limiting defrost clustering while keeping units independent is key to improving system-level heating resilience. However, even for the System A (tightly constrained configuration), statistical analysis showed that SDR > 15% occurred in approximately 0.70% of the operational period, while SDR > 25% occurred in less than 0.16% of the time, indicating that although impactful, such events are relatively infrequent.

Although indoor temperature sensors were not deployed in this study, the observed supply-water temperature fluctuations (ΔT up to 4K) under high SDR conditions suggest potential impacts on indoor thermal comfort, especially in systems with low thermal inertia (e.g., radiator systems). Future studies should incorporate room temperature monitoring to quantitatively assess the relationship between SDR and indoor temperature stability.

Decentralized defrost control should address three levels: (1) temporal—use adaptive delays and state recognition to stagger unit defrosts; (2) spatial—allocate defrost weight dynamically based on module topology and supply–return temperature differences; (3) system intelligence—apply machine learning or data-driven models to predict frosting risk and optimize triggers.

Buffer tank volume, system inertia, and temperature response affect defrost disturbance propagation. Integrated simulation of unit states and hydraulics can quantify these effects and guide adaptive control. Overall, optimization should shift from single-unit, passive defrosting to coordinated, predictive group-level strategies, achieving dispersed defrost loads and enhanced thermal stability.

4. Conclusions

(1) Field measurements of a small-capacity modular ASHP system show that when RH > 80% and compressor frequency > 70 Hz, even short-term defrosting can significantly reduce heating capacity.

(2) Under uncoordinated operation, group defrosting can cluster periodically, with SDR peaks over 60%, causing supply-water temperature fluctuations above 4K.

(3) Heating stability is roughly linearly and negatively correlated with SDR. Keeping SDR below 15% for high-density defrosts and below 60% for transient defrosts limits temperature fluctuations to within 3K.

(4) This highlights the need and design boundaries for decentralized group defrost control. Future strategies should use staggered timing, dynamic module coordination, and predictive algorithms to optimize defrost distribution, enhancing system heating resilience and comfort.

Acknowledgements

This research is supported by the “National Key R&D Program of China [No. 2024YFC3810000]”, “Low Carbon Cities Program of Energy Foundation China (G-2507-36619)”. The authors are grateful for the support of these sponsors.

References

[1] Li, Z. L., Zhang, C. L., Liu, H. M., & Wang, X. C. (2024). Feasibility analysis of thermal storage defrosting method for air source heat pump: From energetic and economic viewpoints. Applied Thermal Engineering, 236, 121828.

[2] Yang, B., Dong, J., Zhang, L., Song, M., Jiang, Y., & Deng, S. (2019). Heating and energy storage characteristics of multi-split air source heat pump based on energy storage defrosting. Applied Energy, 238, 303-310.

[3] Tang, L., Liu, X. A., He, S., & Li, Q. (2024). Performance of an air-source heat pump with multi-circuit outdoor coil for continuous heating during defrosting. Journal of Building Engineering, 85, 108739.

[4] Zheng, C., You, S., Zhang, H., Liu, Z., Zheng, W., & Wu, Z., et al. (2020). Defrosting performance improvement of air-source heat pump combined refrigerant direct-condensation radiant floor heating system with phase change material. Energies, 13.

[5] Zhang, L., Dong, J., Jiang, Y., Deng, S., & Huang, S. (2018). An experimental study on frosting and defrosting performances of a novel air source heat pump unit with a radiant-convective heating terminal. Energy and Buildings, 163, 10-21.

[6] Wei, P., Wang, Z., Feng, H., Wang, S., & Fan, J. (2023). Frost suppression performance of an air source heat pump using sensible heat from indoor air to preheat outdoor air. Building Services Engineering Research & Technology, 44(5), 537-555.

[7] Wu, C., Wang, Z., Li, X., Xu, Z., Xu, C., Yang, Y., ... & Wang, Y. (2023). Field experimental research on retarding frosting and improving defrosting performance of air source heat pumps through variable frequency technology. Journal of Building Engineering, 64, 105628.

[8] Tang, R., Wei, W., Sun, P., Zhao, J., Wang, W., Sun, Y., & Deng, S. (2025). A novel time-current-temperature difference (TIT) defrosting control method for air source heat pump based on outdoor fan operation characteristics in space heating. Applied Thermal Engineering, 259, 124850.

[9] Song, M., Wang, Z., Mao, N., Dong, J., & Zhang, H. (2019). Defrosting start control strategy optimization for an air source heat pump unit with the frost accumulation and melted frost downwards flowing considered. Sustainable Cities and Society, 46, 101461.

[10] Miao, H., Yang, X., Yin, D., Zheng, W., Zhang, H., Zhang, S., & Liu, Z. (2022). A novel defrosting control strategy with image processing technique and fractal theory. International Journal of Refrigeration, 138, 259-269.

[11] Wang, W., Zhou, Q., Tian, G., Wang, Y., Zhao, Z., & Cao, F. (2021). A novel defrosting initiation strategy based on convolutional neural network for air-source heat pump. International Journal of Refrigeration, 128, 95-103.

[12] Ikram, H., Ali, J., Alexander, A., & Bach, C. K. (2025). Optimal heat pump defrosting strategies for full-cycle capacity and COP maximization. Energy, 138302.

[13] Ma, J., Kim, D., Braun, J. E., & Horton, W. T. (2023). Development and validation of a dynamic modeling framework for air-source heat pumps under cycling of frosting and reverse-cycle defrosting. Energy, 272, 127030.

[14] Du, Y., Wu, J., Wang, C., Chen, R., & Li, J. (2020). Investigation on the influence of EEV opening on the reliability of an R290 ASHP during defrosting. Energy and Buildings, 223, 110218.

[15] Wang, W., Di, H., Tang, R., Wei, W., Sun, Y., & Dai, C. (2025). Effect of supply water temperature on frosting performance of air source heat pump and indoor thermal environment in space heating. Building and Environment, 267, 112258.

[16] Song, M., Deng, S., Dang, C., Mao, N., & Wang, Z. (2018). Review on improvement for air source heat pump units during frosting and defrosting. Applied energy, 211, 1150-1170.

[17] Ma, L., Sun, Y., Wang, F., Wang, M., Zhang, S., & Wang, Z. (2025). Advancements in anti-frosting and defrosting techniques for air source heat pumps: A comprehensive review of recent progress. Applied Energy, 377, 124358.